



Short communication

Effects of atmospheric Ti (III) reduction on Nb₂O₅-doped Li₄Ti₅O₁₂ anode materials for lithium ion batteries

Seul-Ki Kim^{a,1}, Eun-Seok Kwon^{a,b,1}, Tae-Heui Kim^b, Jooho Moon^c, Joosun Kim^{a,*}

^aHigh-Temperature Energy Materials Research Center, KIST, Seoul 136-791, Korea

^bCenter of Green Energy Materials Technology, School of Advanced Materials Engineering, Andong National University, Andong 760-749, Korea

^cDepartment of Materials Science and Engineering, Yonsei University, Seoul 120-749, Korea

Received 28 November 2013; received in revised form 25 December 2013; accepted 26 December 2013

Available online 3 January 2014

Abstract

The effects of atmospheric annealing on electrochemical performance for Nb₂O₅-doped Li₄Ti₅O₁₂ anode materials have been investigated. The annealing of Nb₂O₅-doped Li₄Ti₅O₁₂ in Ar-gas suppressed the capacity fade, under the condition of a high charge-discharge rate, by virtue of an enhanced exchange reaction at the electrode/electrolyte interface. Under Ar-gas, Nb₂O₅-doped Li₄Ti₅O₁₂ was primarily reduced to increase the density of Ti³⁺ ions. This caused expansion of the Li₄Ti₅O₁₂ lattice, but had little impact on Li-ion diffusion into the lattice. When concurrent doping and annealing induced such compositional and electrical modification of Li₄Ti₅O₁₂, the polarization resistance of exchange reactions at the electrode/electrolyte interface decreased. Therefore, we have demonstrated that annealing in Ar-gas is capable of decreasing the resistance of exchange reactions at the electrode/electrolyte interface.

© 2014 Elsevier Ltd and Techna Group S.r.l. All rights reserved.

Keywords: Exchange reaction; Li ion battery; Atmospheric annealing; Nb₂O₅; Li₄Ti₅O₁₂

1. Introduction

Lithium-ion batteries are popular, generic power sources for wireless telephones, laptop computers and many other electronic devices. Recently, these batteries have been utilized for applications requiring high energy, high power density and a long lifecycle [1]. Spinel type anode material (e.g., Li₄Ti₅O₁₂–LTO), in particular, is an interesting material expected to have an unlimited life-cycle and to place zero-strain on the lithium host. For these reasons, it is considered a very good alternative to conventional graphite anodes. LTO also has a very flat voltage plateau (about 1.5 V) with respect to the lithium, which corresponds to higher reduction potential than for most organic electrolytes. However, LTO does suffer from limited electric conductivity; which results low rate capacity of a cell.

In order to improve this conductivity, various methods have been proposed: (1) modifying the synthesis route to obtain nano-sized particles (small particle size provides a short

diffusion path for lithium-ion and broad-surface contact between the electrode and electrolyte) [2–9]; (2) adding additional conductive phases (e.g., metals and carbon) into the LTO [10–16]; and (3) substituting other metal oxidizers (e.g., Al³⁺, Ta⁵⁺, Nb⁵⁺, Cr³⁺, Mn⁴⁺, or Mo⁶⁺) for Li or Ti [17–23]. The substitution-induced transition from Ti⁴⁺ to Ti³⁺ in LTO will lead to an increase in its electronic conductivity and thus improve the rate performance. The interesting point is that most of the aforementioned approaches included post-annealing in a reducing atmosphere, possibly enhancing the conductivity. It should be noted that the thermodynamic consideration related to defect formation induced by atmospheric reduction at high temperature, is still valid for the electrodes of Li-ion batteries that operate at room temperature. Vacancy formation and electrovalence maintenance can occur in the aliovalent-dopant-incorporated materials. In this study, we report the effects of post-annealing on the electronic and ionic conduction of Nb₂O₅-doped, LTO anode materials. The results are compared to Nb₂O₅-doped LTO without post-annealing, to understand charge transfer under reducing conditions. Finally, we demonstrate that a combined approach including both Nb₂O₅ doping and post-annealing

*Corresponding author. Tel.: +82 2 958 5528; fax: +82 2 958 5529.

E-mail address: joosun@kist.re.kr (J. Kim).

¹These authors contributed equally to this work.

gives LTO a better rate performance. This revealed the mechanism of enhancement in the context of the charge transfer reaction.

2. Experimental

Using a solid-state method, $\text{Li}_4\text{Ti}_5\text{O}_{12}$ (LTO) and 0.25 mol %- Nb_2O_5 doped $\text{Li}_4\text{Ti}_5\text{O}_{12}$ (Nb-LTO) samples were prepared from Li_2CO_3 (99%, Sigma-Aldrich), TiO_2 (99.9%, Aldrich), and Nb_2O_5 (99.9%, High Purity Chemicals, Japan). A 0.25 mol% (of Nb_2O_5) doping level was selected to yield the composition of $\text{Li}_4\text{Ti}_{4.995}\text{Nb}_{0.005}\text{O}_{12}$. Stoichiometric ingredients were mixed by ball-milling for 24 h and then dried at 80 °C for 12 h. The dried powders were calcined at 850 °C for 12 h in air. Post-annealing was performed at 800 °C for 24 h under argon gas using the calcined powder.

The crystal structure and lattice parameters of the synthesized powders were identified by X-ray diffraction (XRD, CuK_α , PW3830, PANalytical, Netherlands). The surface morphologies were examined using scanning electron microscopy (SEM, XL30 ESEM, Philips, Netherlands). X-ray photoelectron spectroscopy (XPS, PHI-5000 VersaProbe, Ulvac-PHI, Japan) was used to investigate the various surface chemical structures resulting from doping and Ar-gas annealing. Using a multi-meter (2000, Keithley) and precision current source (6220, Keithley), four-probe DC conductivities were determined for bar-shaped samples prepared by 5 wt% of PVB (polyvinyl-butylal, Aldrich) addition and subsequent sintering under the same conditions as for preparation of the powdered ingredients. Electrochemical characterizations were realized in CR2032 type coin cells, using 20 mg of active materials (LTO or Nb-LTO) and 12 mg of TAB (teflonized acetylene black) in NMP (N-methylpyrrolidone). The prepared mixtures were then pressed onto Ni mesh and finally dried at 120 °C for 12 h under vacuum in order to remove the solvent. Coin cells were assembled in an Ar-filled glove box where the O_2 and H_2O content was less than 1 ppm. The electrolyte used was a mixture of 1 M LiPF_6 -ethylene carbonate (EC) and diethyl carbonate (DEC-1:1 by volume; OSAKA Kisida Chemical, Japan). All the electrochemical tests were performed using lithium (Sigma-Aldrich, 99.9%) counter electrodes. Charge-discharge measurement at room temperature was carried out using a battery test system (N174-HR, Toyo, Japan) with cut-off voltage of 0.5–2.3 V at various constant current densities (0.2–2 C). Impedance spectra were also measured by means of an impedance analyzer (SI1287 and 1260, Solartron, USA). The frequency was varied from 5 mHz to 100 kHz.

3. Results and discussion

Fig. 1 shows the microstructures of LTO and of 0.25 mol% of Nb_2O_5 -doped-LTO calcined at 850 °C for 12 h. The powders exhibited a uniform size-distribution without any severe agglomeration or significant change in particle size for both pure LTO (**Fig. 1a**) and Nb_2O_5 -doped LTO (**Fig. 1b**). The measured average particle size was $\sim 0.5 \mu\text{m}$. Through the additional X-ray diffraction analysis, both powders were

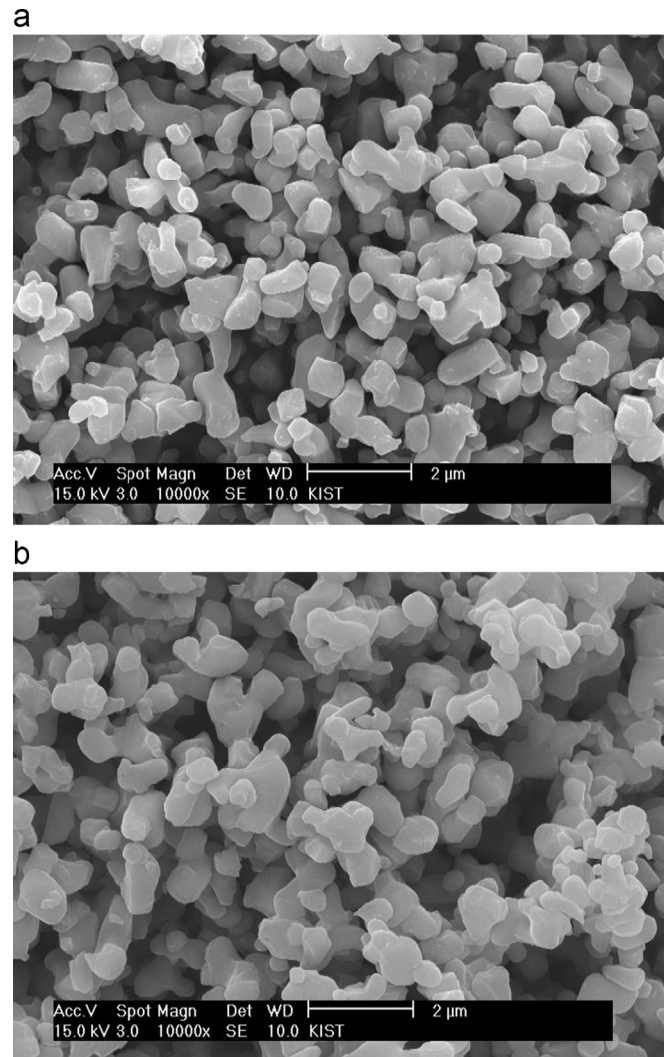


Fig. 1. Microstructures of (a) $\text{Li}_4\text{Ti}_5\text{O}_{12}$ and (b) 0.25 mol% Nb_2O_5 -doped $\text{Li}_4\text{Ti}_5\text{O}_{12}$ calcined at 850 °C for 12 h in air.

indexed to LTO cubic spinel structures (JCPDS 26-1198) and showed no additional characteristic peaks corresponding to any secondary phase, indicating Nb_2O_5 doping into the spinel lattice as shown in **Fig. S1** (Supplementary information).

X-ray diffraction refinement by the least-mean-square method revealed that the lattice parameter expands only for the doped sample after post-annealing under Ar-gas, as shown in **Table 1**. Three other samples, pure LTOs with and without annealing, and even Nb_2O_5 -doped LTO without annealing; however, exhibited almost the same lattice parameters, which is in good agreement with previously reported values of LTO prepared under atmospheric air [24,25]. Little of the impact of Nb_2O_5 doping on the lattice parameter change in our experiment is due to the swallow level of doping. The large expansion reported in other research would result only from heavy doping; meaning orders of magnitude higher than this study [20]. According to variation in the lattice parameter of the samples, the lattice volume expansion for 0.25 mol% Nb_2O_5 -doped LTO was negligible compared to that of undoped LTO; however, the Ar-gas annealing induced a

Table 1
Lattice parameters of as-synthesized and full-charged LTOs.

Sample	Annealing atmosphere	As-synthesized (Å)	At charged (Å)
LTO	—	8.3578 ± 0.0009	8.3641 ± 0.0016
	Ar	8.3579 ± 0.0008	8.3644 ± 0.0039
Nb-LTO	—	8.3583 ± 0.0007	8.3633 ± 0.0038
	Ar	8.3611 ± 0.0014	8.3680 ± 0.0026

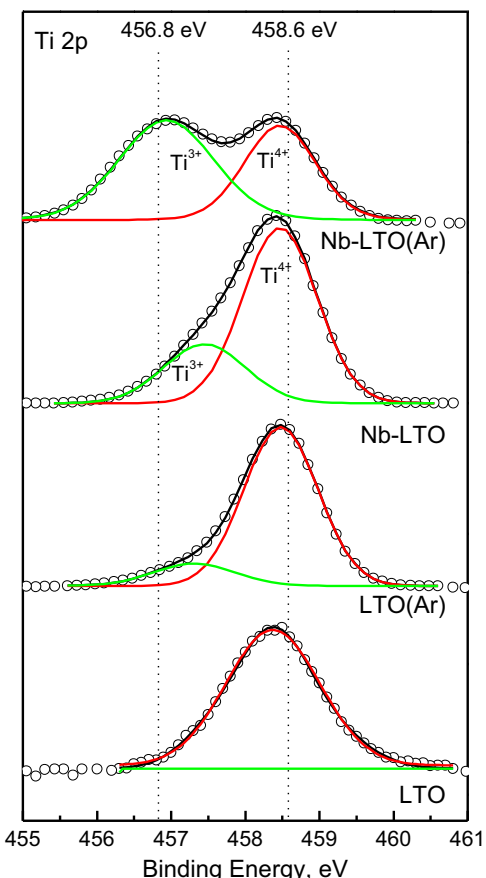


Fig. 2. XPS spectra of $\text{Li}_4\text{Ti}_5\text{O}_{12}$, Ar-annealed $\text{Li}_4\text{Ti}_5\text{O}_{12}$, 0.25 mol% Nb_2O_5 -doped $\text{Li}_4\text{Ti}_5\text{O}_{12}$, and Ar-annealed 0.25 mol% Nb_2O_5 -doped $\text{Li}_4\text{Ti}_5\text{O}_{12}$.

significant change amounting to $\sim 1\%$. The lattice expansion of doped-LTO after annealing might have resulted because (1) the ionic radius of foreign Nb^{5+} (0.64 \AA) is larger than that of host Ti^{4+} (0.605 \AA), or (2) excess electrons produced by donor doping caused the valence transition from existing Ti^{4+} to Ti^{3+} (0.67 \AA) by means of charge compensation [26]. We suggest that these two mechanisms are activated by atmospheric annealing, and in particular, that transition from Ti^{4+} to Ti^{3+} plays a major role.

To confirm the Ti-ion valence state of the Nb_2O_5 -doped LTO and Ar annealed sample, XPS was conducted and shown in Fig. 2. For 0.25 mol% Nb_2O_5 -doped and Ar-annealed sample, the Ti 2p_{3/2} spectrum was clearly decomposed to sub-peaks with binding energy of 456.8 and 458.6 eV, which were assigned to Ti^{3+} and Ti^{4+} ions, respectively. However,

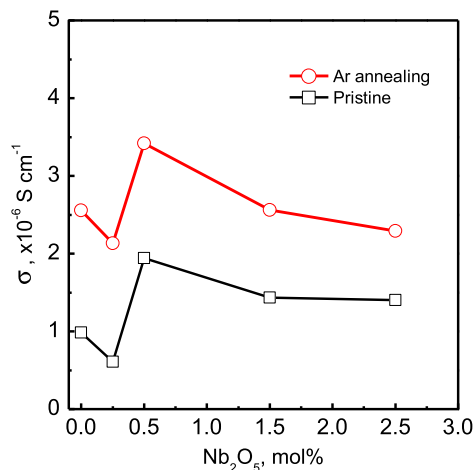


Fig. 3. Electrical conductivities of pristine and Ar-annealed $\text{Li}_4\text{Ti}_5\text{O}_{12}$ samples as a function of Nb_2O_5 doping.

other samples only showed a shoulder corresponding to trace amounts of Ti^{3+} ion. These results support the notion that reducing gas annealing activates the transition from Ti^{4+} to Ti^{3+} ion only when the LTO has been doped with Nb_2O_5 . Such differences in XPS spectra, depending on the sample treatment conditions, originated from the swallow doping level as well as the extent of surface segregation of the external doping species. Heavy doping, in this case, generates a large amount of excess electrons; enough to reduce Ti^{4+} to Ti^{3+} , which overwhelms the contribution of reducing gas annealing [27]. Annealing under Ar-gas cannot significantly reduce the oxygen partial pressure so that such an activation effect is unable to be observed for the heavily doped LTO.

Following the charge neutrality condition, Nb_2O_5 doping into LTO replaces Ti^{4+} with Nb^{5+} ions, generating Nb_{Ti} defect (in term of Kröger-Vink notation). This promotes electrical conductivity and lattice expansion, but has little impact on the samples at a swallow-level of doping. Additional Ar-annealing; however, nonstoichiometric charge-neutrality condition ($[e'] = 2[V_{\text{o}}^{\cdot}]$) produces surplus of Ti^{4+} to Ti^{3+} ion transitions; resulting in high electronic conductivity and lattice expansion. The swallow level of Nb_2O_5 -doping was confirmed by measuring the electric conductivity as a function of Nb_2O_5 doping-amount. Fig. 3 shows that the electrical conductivities of 0.25 mol% of Nb_2O_5 doped LTO samples exhibited minimum values regardless of the details of annealing conditions. This indicates that the doping level we selected, was proper to signify the effects of atmospheric annealing.

Combining the effects of the lattice expansion and the Ti-ion reduction likely increased the Li-ions as well as the electron conduction of the LTO adapted for use as anode materials in Li-ion batteries.

Furthermore, the sample annealed in Ar showed superior conductivity compared with pristine samples over the entire doping range, indicating the possibility that LTO-anodes without conducting media such as carbon-derived additives could be used for Li-ion battery compartments. Song et al. [28] reported that the high capacity of carbon-free LTO electrodes, when annealed in a reducing atmosphere is owed to the partial reduction of Ti^{4+} and surface metallic $Li_7Ti_5O_{12}$. We therefore confirmed that the exceptional conductivity of carbon-free LTO anode materials is valid only for those annealed in a reducing atmosphere. An interesting point is shown in Table 1: that persistent lattice expansion is observed for the doped and Ar-annealed LTO; even after reaching a fully-charged condition. Such a sustainable structure implies not only a high rate of capacity retention over long-term battery operation, but also high-rate capability under conditions of fast charge-discharge cycles.

Discharge rate capabilities of the samples were investigated by increasing the applied specific current every 10 cycles and shown in Fig. 4a. A 0.25 mol% Nb_2O_5 -doped and subsequently Ar-annealed LTO sample exhibited the highest rate capability (over 1 C), compared with the other LTOs. Initial specific capacities of 185 mA h/g, 150 mA h/g, 110 mA h/g, 62 mA h/g, were obtained for applied specific currents of

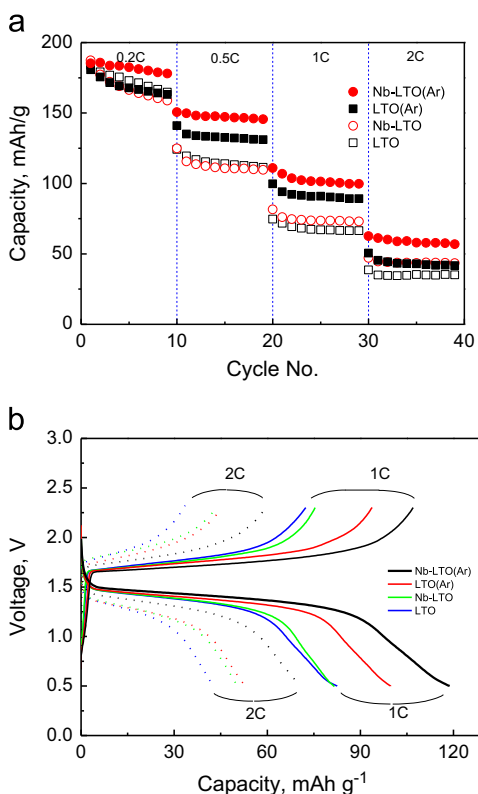


Fig. 4. (a) Specific capacities cycled at various rates from 0.2 to 2 C, and (b) charge and discharge curves at rates of 1 and 2 C for $Li_4Ti_5O_{12}$ samples.

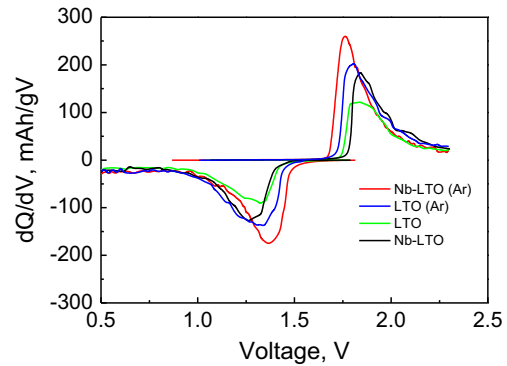


Fig. 5. Differential capacity vs. voltage plots for various $Li_4Ti_5O_{12}$ samples in the second cycle between 0 and 2.3 V.

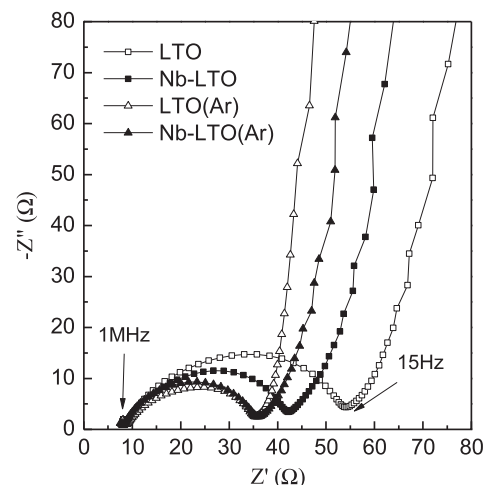


Fig. 6. Impedance measurements for $Li_4Ti_5O_{12}$ samples. Post-annealed LTOs in Ar atmosphere show low charge transfer resistances.

35 mA/g (0.2 C), 88 mA/g (0.5 C), 175 mA/g (1C), and 350 mA/g (2C), respectively. This agreed with our expectation that the doped and Ar-annealed sample would likely show the best electrochemical performance, considering the measured electrical conductivity and the reduction behavior of Ti-ion; as confirmed by XPS results. The discharge voltage plateau of every sample decreased with increasing current rate, and its plateau-spans also shrunk. Eventually (at 2 C), no obvious plateau region was observed. For the 0.25 mol% Nb_2O_5 -doped and Ar-annealed sample; however, an obvious discharge plateau was still observed even when the current rate was 2 C, exhibiting an excellent rate capability (Fig. 4b). This means that Ar-gas post-annealing allows for enhanced Li-ion diffusion and electronic conductivity by Nb_2O_5 doping. As shown in Fig. S2 (Supplementary information), this annealing effect still holds at long-term cyclic operation.

Fig. 5 shows the differential capacity curves of LTO samples in the second cycle; between 0 and 2.3 V. All the curves show one cathodic-peak located at about 1.3 V (vs. Li/Li⁺); corresponding to the Li intercalation, and another anodic-peak located at about 1.7 V (vs. Li/Li⁺); corresponding

Table 2

Charge transfer resistances at electrode/electrolyte interface and Li-ion diffusivities of LTO samples.

Sample	Annealing atmosphere	Charge transfer resistance (Ω)	Li-ion diffusivity (cm^2/s)
LTO	—	48.1	4.8×10^{-9}
	Ar	27.8	3.2×10^{-9}
Nb-LTO	—	38.8	8.4×10^{-9}
	Ar	28.1	4.1×10^{-9}

to Li de-intercalation from spinel LTO structures. Even though all the peaks exhibited similar shapes, peak heights increased sequentially in the order of LTO, Nb-LTO, LTO Ar-annealed, and Nb-LTO Ar-annealed samples. The differences in potential between the anode and cathode-peaks also decreased in the same order. The 0.25 mol% of Nb_2O_5 -doped and Ar-annealed sample; therefore, possessed the lowest polarization of charge transfer reaction and the highest diffusivity of lithium ion inside the electrode. To clarify the extent of the two contributions above, measured EIS results were fitted based on an equivalent circuit model. As shown in Fig. 6, the semicircle in the high frequency region represents the transfer of the lithium ions at the electrode/electrolyte interface, and the next straight line at low frequencies corresponds to the diffusion of lithium ions into the electrode materials (Warburg diffusion) [20,29]. We selected the typical equivalent model for LTO and followed the suggested procedures. The detailed information for the modeling and fitting can be found elsewhere [20]. The measured polarization resistance related with the charge transfer at the electrode/electrolyte interface of Nb_2O_5 doped and Ar-annealed sample showed minimum values. However, there was no difference in Li-ion diffusivity into the LTO electrode regardless of doping and atmospheric annealing (see Table 2). The lattice expansion did not contribute to Li-ion diffusion into the active materials, indicating that the enhanced performance at high current rates is not due to enhanced Li-ion diffusion. Considering this, we suggest that the enhanced electrochemical performance after the sample was doped and annealed under Ar-gas resulted in the promotion of charge transfer reactions at the electrode/electrolyte interface.

4. Conclusions

A powder of 0.25 mol% Nb_2O_5 doped $\text{Li}_4\text{Ti}_5\text{O}_{12}$ (LTO) was synthesized using a solid-state method and then post-annealed in Ar-gas. Nb_2O_5 swallow-doping and subsequent Ar-annealing of LTO induces the transition from Ti^{4+} to Ti^{3+} , which increases the charge transfer reaction, and in turn contributes to the enhancement of battery performance. The increased Ti^{3+} -ion density makes the LTO lattice expand; however, it has little impact on Li-ion diffusion into the lattice. Ar-gas annealing is capable of decreasing the resistance of exchange reaction at the electrode/electrolyte interface only when there is concurrent aliovalent doping and reduction annealing of LTO.

Acknowledgment

This work was supported by a National Research Foundation of Korea Grant (NRF-2010-C1AAA001-2010-0028971) funded by the Korean Government (MEST).

Appendix A. Supplementary information

Supplementary data associated with this article can be found in the online version at <http://dx.doi.org/10.1016/j.ceramint.2013.12.132>.

References

- [1] K. Ariyoshi, Y. Makimura, T. Ohzuku, Lithium insertion materials having spinel-framework structure for advanced batteries, in: K. Ozawa (Ed.), *Lithium Ion Rechargeable Batteries: Materials, Technology, and New Applications*, Wiley-VCH, Weinheim, 2009 (pp. 11).
- [2] C.H. Jiang, M. Ichihara, I. Honma, H.S. Zhou, Effect of particle dispersion on high rate performance of nano-sized $\text{Li}_4\text{Ti}_5\text{O}_{12}$ anode, *Electrochim. Acta* 52 (2007) 6470–6475.
- [3] D. Wang, H.Y. Xu, M. Gu, C.H. Chen, $\text{Li}_2\text{CuTi}_3\text{O}_8\text{-Li}_4\text{Ti}_5\text{O}_{12}$ double spinel anode material with improved rate performance for Li-ion batteries, *Electrochim. Commun.* 11 (2009) 50–53.
- [4] A. Guerfi, P. Charest, K. Kinoshita, M. Perrier, K. Zaghib, Nano electronically conductive titanium-spinel as lithium ion storage negative electrode, *J. Power Sources* 126 (2004) 163–168.
- [5] P.G. Bruce, B. Scrosati, J.M. Tarascon, Nanomaterials for rechargeable lithium batteries, *Angew. Chem. Int. Ed.* 47 (2008) 2930–2946.
- [6] Y.F. Tang, L. Yang, Z. Qiu, J.S. Huang, Preparation and electrochemical lithium storage of flower-like spinel $\text{Li}_4\text{Ti}_5\text{O}_{12}$ consisting of nanosheets, *Electrochim. Commun.* 10 (2008) 1513–1516.
- [7] C.H. Jiang, Y. Zhou, I. Honma, T. Kudo, H.S. Zhou, Preparation and rate capability of $\text{Li}_4\text{Ti}_5\text{O}_{12}$ hollow-sphere anode material, *J. Power Sources* 166 (2007) 514–518.
- [8] E. Matsui, Y. Abe, M. Senna, Solid-State synthesis of 70 nm $\text{Li}_4\text{Ti}_5\text{O}_{12}$ particles by mechanically activating intermediates with amino acids, *J. Am. Ceram. Soc.* 91 (2008) 1522–1527.
- [9] Y.J. Hao, Q.Y. Lai, D.Q. Liu, Z.U. Xu, X.Y. Ji, Synthesis by citric acid sol-gel method and electrochemical properties of $\text{Li}_4\text{Ti}_5\text{O}_{12}$ anode material for lithium-ion battery, *Mater. Chem. Phys.* 94 (2005) 382–387.
- [10] S.H. Huang, Z.Y. Wen, J.C. Zhang, X.L. Yang, Improving the electrochemical performance of $\text{Li}_4\text{Ti}_5\text{O}_{12}/\text{Ag}$ composite by an electroless deposition method, *Electrochim. Acta* 52 (2007) 3704–3708.
- [11] H.Y. Yu, X.F. Zhang, A.F. Jalbout, X.D. Yan, X.M. Pan, H.M. Xie, R.S. Wang, High-rate characteristics of novel anode $\text{Li}_4\text{Ti}_5\text{O}_{12}$ /polyacene materials for Li-ion secondary batteries, *Electrochim. Acta* 53 (2008) 4200–4204.
- [12] R. Dominko, M. Gaberscek, M. Bele, D. Mihailovic, J. Jamnik, Carbon nanocoatings on active materials for Li-ion batteries, *J. Eur. Ceram. Soc.* 27 (2007) 909–913.

- [13] H. Liu, Y. Feng, K. Wang, J.Y. Xie, Synthesis and electrochemical properties of $\text{Li}_4\text{Ti}_5\text{O}_{12}/\text{C}$ composite by the PVB rheological phase method, *J. Phys. Chem. Solids* 69 (2008) 2037–2040.
- [14] S.H. Huang, Z.Y. Wen, B. Lin, J.D. Han, X.G. Xu, The high-rate performance of the newly designed $\text{Li}_4\text{Ti}_5\text{O}_{12}/\text{Cu}$ composite anode for lithium ion batteries, *J. Alloys Compd.* 457 (2008) 400–403.
- [15] J.J. Huang, Z.Y. Jiang, The preparation and characterization of $\text{Li}_4\text{Ti}_5\text{O}_{12}$ /carbon nano-tubes for lithium ion battery, *Electrochim. Acta* 53 (2008) 7756–7759.
- [16] D.T. Liu, C. Ouyang, J. Shu, J. Jiang, Z.X. Wang, L. Chen, Theoretical study of cation doping effect on the electronic conductivity of $\text{Li}_4\text{Ti}_5\text{O}_{12}$, *Phys. Status Solidi (B)* 243 (2006) 1835–1841.
- [17] D. Capsoni, M. Bini, V. Massarotti, P. Mustarelli, S. Ferrari, G. Chiodelli, M.C. Mozzati, P. Galinetto, Cr and Ni doping of $\text{Li}_4\text{Ti}_5\text{O}_{12}$: cation distribution and functional properties, *J. Phys. Chem. C* 113 (2009) 19664–19671.
- [18] J.P. Zhu, J.J. Zhao, Q.S. Wang, H.W. Yang, G. Yang, Effects of aluminum doping on the performance of lithium ion battery material $\text{Li}_4\text{Ti}_5\text{O}_{12}$, *Adv. Sci. Lett.* 4 (2011) 474–476.
- [19] J. Wolfenstine, J.L. Allen, Electrical conductivity and charge compensation in Ta doped $\text{Li}_4\text{Ti}_5\text{O}_{12}$, *J. Power Sources* 180 (2008) 582–585.
- [20] B.B. Tian, H.F. Xiang, L. Zhang, Z. Li, H.H. Wang, Niobium doped lithium titanate as a high rate anode material for Li-ion batteries, *Electrochim. Acta* 55 (2010) 5453–5458.
- [21] Z.X. Long, H.G. Rong, P.Z. Dong, Preparation and effects of Mo-doping on the electrochemical properties of spinel $\text{Li}_4\text{Ti}_5\text{O}_{12}$ as anode material for lithium ion battery, *J. Inorg. Mater.* 26 (2011) 443–448.
- [22] H. Zhao, Y. Li, Z.M. Zhu, J. Li, Z.H. Tian, R. Wang, Structural and electrochemical characteristics of $\text{Li}_{4-x}\text{Al}_x\text{Ti}_5\text{O}_{12}$ as anode material for lithium-ion batteries, *Electrochim. Acta* 53 (2008) 7079–7083.
- [23] X. Li, M. Qu, Z. Yu, Structural and electrochemical performances of $\text{Li}_{4\text{Ti}_{5-x}\text{Zr}_x\text{O}_{12}}$ as anode material for lithium-ion batteries, *J. Alloys Compd.* 487 (2009) L12–L17.
- [24] S. Huang, Z. Wen, Z. Gu, X. Zhu, Preparation and cycling performance of Al^{3+} and F^- co-substituted compounds $\text{Li}_4\text{Al}_x\text{Ti}_{5-x}\text{F}_y\text{O}_{12-y}$, *Electrochim. Acta* 50 (2005) 4057–4062.
- [25] M.R. Harrison, P.P. Edwards, J.B. Goodenough, The superconductor-semiconductor transition in the $\text{Li}_{1+x}\text{Ti}_{2-x}\text{O}_4$ spinel system, *Philos. Mag. B* 52 (1985) 679–699.
- [26] R.D. Shannon, Revised effective ionic radii and systematic studies of interatomic distances in halides and chalcogenides, *Acta Cryst. A* 32 (1976) 751–767.
- [27] J. Wolfenstine, U. Lee, J.L. Allen, Electrical conductivity and rate-capability of $\text{Li}_4\text{Ti}_5\text{O}_{12}$ as a function of heat-treatment atmosphere, *J. Power Sources* 154 (2006) 287–289.
- [28] M.S. Song, a. Benayad, Y.M. Choi, K.S. Park, Does $\text{Li}_4\text{Ti}_5\text{O}_{12}$ need carbon in lithium ion batteries? Carbon-free electrode with exceptionally high electrode capacity, *Chem. Commun.* 48 (2012) 516–518.
- [29] T.F. Yi, Y. Xie, L.J. Jiang, J. Shu, C.B. Yue, A.N. Zhou, M.F. Ye, Advanced electrochemical properties of Mo-doped $\text{Li}_4\text{Ti}_5\text{O}_{12}$ anode material for power lithium ion battery, *RSC Adv.* 2 (2012) 3541–3547.